SAND2000-1630J

CHARACTERISTICS AND MECHANISMS IN ION-CONDUCTING POLYMER FILMS AS CHEMICAL SENSORS

RECEIVED
AUG 17 2000
OSTI

R. C. Hughes*, W. G. Yelton, K. B. Pfeifer, and S. V. Patel

Microsensor Dept., Sandia National Laboratories, Albuquerque, NM, 87185

ABSTRACT

Solid Polymer Electrolytes (SPE) are widely used in batteries and fuel cells because of the high ionic conductivity that can be achieved at room temperature. The ions are usually Li or protons, although other ions can be shown to conduct in these polymer films. There has been very little published work on SPE films used as chemical sensors. We have found that thin films of polymers like polyethylene oxide (PEO) are very sensitive to low concentrations of volatile organic compounds (VOCs) such as common solvents. Evidence of a new sensing mechanism involving the percolation of ions through narrow channels of amorphous polymer is presented. We will present impedance spectroscopy of PEO films in the frequency range 0.0001 Hz to 1 MHz for different concentrations of VOCs and relative humidity. We find that the measurement frequency is important for distinguishing ionic conductivity from the double layer capacitance and the parasitic capacitance.

Keyword: Polyethylene Oxide; PEO; Polyethylene glycol; impedance spectroscopy; ionic conductor; chemical sensor; solid polymer electrolyte; conduction mechanism

*Corresponding author: Sandia National Laboratories, P.O. Box 5800, MS-1425, Albuquerque, NM, 87185, email: rchughe@sandia.gov, fax: (505) 844-1198

Introduction

There is a rich literature on the electrical properties of polyethylene oxide (PEO) because of its importance as an electrolyte in lithium batteries.[1,2] However, there have been relatively few reports of its use as a sensor material.[3] Much of the reported work on PEO as an electrolyte involves attempts to increase the ionic mobility without the use of water because of the incompatibility with lithium. Plasticizing agents and non-aqueous electrolytes like propylene carbonate are often used to increase the room temperature ionic conductivity.[1] In this paper we report on the chemical sensing characteristics and mechanism of thin films of PEO doped with $LiClO_4$ deposited on planar arrays of interdigitated electrodes. The planar configuration allows easy integration with sensing electronics and fast response to vapor phase analytes. An unusual pattern of relative responses to vapors with different solubility parameter values[4], makes PEO a useful addition to arrays of chemiresistors used in pattern recognition of vapors and mixtures of vapors. We will discuss the issues of the mixed crystalline and amorphous polymer phases, as well as, the temperature dependence of the chemical sensor responses.

Experimental

The PEO was purchased from Polysciences and had a nominal molecular weight (MW) of 4,000,000 g/mol. The $LiClO_4$ was purchased from Aldrich Chemical and both components were dissolved in acetonitrile, mixed and deposited onto planar interdigitated electrode (IDE) arrays. Polyethylene glycol (short chain PEO) in two different molecular weights (PEG68 has molecular weight of 6800 g/mol and PEG34, 3400 g/mol) was purchased from (Scientific

Polymer Products, Inc.). Carbon loaded PEG films were also fabricated as described in Ref. 4 to make chemiresistors for direct comparison to sensing by ion conductivity in the same type of polymer film.

The 50 pair electrode arrays had 5 μm wide gold lines separated by 10 μm gaps on quartz substrates. A photomicrograph is shown in Fig. 1 of part of the array. The electrode lengths are 0.16 cm. Since the nominal thickness of the polymer films is about 0.5 μm, much less than the gap, parallel plate geometry is a good approximation with an A/d (electrode area over distance between electrodes) of $8 \times 10^{-6}/1 \times 10^{-3} = 8 \times 10^{-3}$ cm. There are 100 resistors in parallel, making the geometrical conversion to the bulk conductivity value in units of $\text{ohm}^{-1}\ \text{cm}^{-1}$ from 1/Z in ohm^{-1}, a factor of 0.8 cm^{-1}. The series resistance of the region close to the electrodes (where it deviates from the parallel plate model) is hard to calculate, but is clearly too small to make more than a 1% difference in the calculation of the bulk conductivity. For polymer films thicker than the 10 micron electrode gap, the extraction of the bulk conductivity becomes analytically more difficult because of the non-uniformity of the electric field lines, however, mathematical models of this behavior are given are given in Ref. 5. The bulk conductivity values, often quoted in the polymer electrolyte literature, are usually measured in sandwich cells (like batteries), but are comparable to our values for the dry electrolyte.

Samples with PEO to $LiClO_4$ ratios from 7:1 to 15:1 (by weight) were fabricated using either spin or drop coating from solutions in acetonitrile. This corresponds to 17:1 to 36:1 in the ratio of O:Li. Samples using the lower molecular weight PEO (called polyethylene glycol, or PEG) were fabricated from water solutions. PEG films loaded with conductive carbon particles to form chemiresistors were also fabricated for comparison using methods described in Refs. 4 and 6. Impedance spectra were taken with a Solartron SI 1260 Impedance/Gain-Phase Analyzer coupled to the 1296 Dielectric Interface. The samples were temperature controlled in an oven and the different vapors were provided by a vapor generation system that used nitrogen as a carrier and dilution gas, and is described elsewhere.[4,6]

Analytes included isooctane, cyclohexane, toluene, trichloroethylene, xylene, DIMP (diisopropylmethylphosphonate), DMMP (dimethylmethylphosphonate), ethanol, methanol, and water. These solvents and analytes were commercially available (Fisher Chemical) and used as received, except ethanol, which was distilled to remove water. In some cases, molecular sieves were added to the bulk solvents to check for water contamination in the sensor signals.

Results

The impedance spectra from polyelectrolytes containing no redox species have the same general characteristics, shown in Fig. 2. We prefer to show the data in the form of log impedance vs. log frequency and the phase in a separate graph, rather than the common Nyquist plot, because we are often trying to identify the best frequency range for sensor operation. A good tutorial on impedance spectra in solid polymer electrolytes is given in Ref. 7. The simulated spectra from a simple lumped circuit, is shown for two cases: the film in dry N_2 at 22°C and in 20% relative humidity. The parasitic capacitance comes mostly from the quartz substrate with a small additive effect from the electric fields in the gas above the electrodes, and the parasitic capacitance dominates the high frequency impedance. The region showing the ionic conductivity is relatively frequency independent in the mid-frequency range and has a phase corresponding to almost pure resistance. It is only values in this frequency region that are used in the calculation of the bulk conductivity described above; the value of Z_{real} (real part of the total impedance) at the minimum phase is used as R_{ionic}. The value of R_{ionic} gives a stronger dependence than C_2 on the concentration of different volatile organic compounds (VOCs). The lowest frequencies show the double layer capacitance (simulated by C_2) on the electrodes; the phase moves towards pure capacitance as the frequency goes lower.

Figures 3a, b and c show the fixed frequency, transient and steady-state response of a PEO7:1 sensor film to pulses of a variety of analytes. In a previous publication[6] we have discussed the use of the analyte solubility parameter in mapping out sensor responses. The pulses of vapors shown in Fig. 3, start with the lowest solubility parameter analyte, isooctane, and proceed in order to the highest, water. In each case 10% of the saturated vapor pressure (at 21°C) is used as the exposure concentration. If there are no special interactions between the analyte molecules and the PEO film, all the signals would be the same size (from entropic considerations). The differences in signal size show the magnitudes of the specific interactions; very weak or repulsive for the low solubility parameter analytes and strong for polar molecules, such as water and methanol, which have high solubility parameters. The organophosphonate molecules, DIMP and DMMP have especially large signals compared to the other molecules with similar solubility parameters. All the data in this figure were taken using a lock-in amplifier coupled to a current amplifier operating at 100 Hz. For the largest signals there is some change in phase at this frequency, indicating that the measured impedance is not quite the ionic conductivity, but has some capacitive component mixed in. The true value for R_{ionic} could be calculated for each point in time using the lumped circuit parameters, but this was not done since we were most interested in the time response of the sensor signal in a simple read-out circuit.

When the sensor films are held at elevated temperatures (3b and 3c), it can be seen that the sizes of the signals are smaller (fractional changes in impedance), but the responses are faster, particularly on the desorption side. The base or dry resistance is also lower because of the enhanced thermal activation of the conductivity in these solid polymer electrolytes. In each case we are holding the gas phase concentration of analyte constant at $p/p_{sat} = 10\%$ (for p_{sat} at 21°C); the responses would be bigger if we used the p_{sat} at the temperature of the sensor.

The large signals from DIMP, for 10% p/p_{sat} or about 100 ppm absolute concentration, led us to look at lower concentrations to see where the limits of detection might be. In Fig. 4, the response to steps of 1 ppm and 0.5 ppm at two sensor temperatures are shown using a chiller (NESLAB Instrument, Inc., model RTE-111) to cool the DIMP bubbler. The estimated vapor pressure for DIMP liquid at 0°C is about 0.06 Torr. The large signal to noise for 1 ppm DIMP means that concentrations in the low ppb's should be detectable.

We have previously published response data on chemiresistors fabricated from composites of polymers with carbon particles.[4,6] Their resistance has little or no frequency dependence, so they are usually measured using DC circuits. In Fig. 5, we show a comparison of an ion conducting chemiresistor and a carbon composite chemiresistor made from the same polymer, in this case a PEG with a molecular weight of 6800 g/mol. The data for the PEG68 (10:1) $LiClO_4$ looks very similar in impedance magnitude and response speed to the higher molecular weight PEO films shown in Fig. 3. In Fig. 5 it can be seen that the relative responses of the two sensors to the different vapors is quite different, especially to trichloroethylene (TCE), DMMP, and methanol. For clarity of comparison, the carbon composite data use $\Delta R/R_0$ normalized to the largest signal for the particular sensor. The analysis for the ion conductor uses $\log(G/G_0)$ where G is the conductance, 1/R. The relative differences for the analytes point to the different mechanisms of detecting the analyte even though both are employing electrical resistance changes.

The temperature dependence of the conductivity for PEO/salt electrolytes appears in many papers and has been the subject of much theoretical analysis.[2] The data for nominally the same type of PEO and concentration of salt varies widely at room temperature, but at the higher temperatures, about 100°C, a limiting high value of about 10^{-3} S/cm seems to be reached in most samples. The technological goal has been to raise the lower-temperature conductivity to this high level. Fig. 6 shows the temperature dependence of two of our PEO samples from 20 to 90°C. It is plotted on the typical log conductivity vs. 1/T plot, but the data does not fit a simple straight line Arrhenius-type behavior. This behavior is typical of the solid electrolytes and results from the complex mechanisms for ion transport in these materials. The impedance of other compositions of the high molecular weight PEO and the PEG lithium ion composites (all semicrystalline) show the same sort of temperature dependence as the semicrystalline sample displayed in Fig. 6. Also shown in Fig. 6 is the high conductivity found for one of the PEO 15:1 samples, which has been made fully amorphous by heating to 140°C and then quenched rapidly to 21°C. After some undetermined period of time the metastable amorphous films will recrystallize, but this particular sample remained amorphous long enough to obtain the reversible temperature dependence of the conductivity as shown in the upper curve and also response data to a variety of analytes.

Fig. 7 shows the temperature dependence of the DC resistance (in the four terminal measurement mode) of the PEG68-30-C sensor. The relative response to various vapors for this sensor was shown in Fig. 5. Increasing temperature leads to a very strong increase in resistance at about 58°C. This thermal response corresponds to the melting temperature of the PEG68 to a clear low viscosity liquid. During the experiment the sensor was held horizontal, however there was no well or depression used to prevent distortion of the shape of the liquid film. Surface tension apparently kept the film about the same shape. The sensor was maintained above the melting temperature for several hours, pausing at 71, 81 and 91°C. On cooling there is strong evidence for supercooling of the liquid before freezing into the solid phase. The sharp increase in resistance on melting is probably due to the large volume change in going to the liquid state. Another temperature cycle using an ac voltage to measure the resistance showed the same general features, although in the liquid region (where the carbon particles are somewhat free to move around), the resistance increased slightly with time instead of the decrease seen in Fig. 7. These data are the first reports of carbon composite chemiresistors measured in the low viscosity melt phase of the polymer.

During the same run, the resistance of the ion-conducting sensor (10:1 $LiClO_4$) from the same PEG68 polymer was monitored at 100 Hz and is shown in Fig. 8. The melting transition has a much smaller effect on the ion conductivity and any supercooling is difficult to observe.

In Fig. 2, the simulated impedance vs. frequency plot shows the effect of the large capacitance, C_2, on the low frequency part of the spectrum. This capacitance is associated with the double layer of ions very near to the gold electrode (within about 10 nm). In Fig. 9, we show the effect of analyte concentration on this low frequency region of the PEO_{10} spectrum for acetonitrile at 21°C. A rough value for C_2 can be obtained from the formula:

$$C = 1/(2\pi f Z), \qquad [1]$$

where f is the frequency in Hz and Z the impedance in ohms. The geometric area of the gold electrodes gives the formula for the capacitance in farads/cm^2: $C_{dl} = C*468$. This takes into account the fact that for each "cell" there is a capacitor on each electrode in series, so the capacitance of each electrode interface is twice the measured capacitance. The calculation gives a value of about 10 microfarads/cm^2 at 0.1 Hz. This value is in line with double layer capacitance values seen in liquid electrolytes.[8] It can be seen that the double layer capacitance (e.g. at 0.1 Hz) is a much weaker function of the analyte concentration than the ionic conductance. The best value for the ionic conductivity is at the frequency where the phase is at a minimum. Ideally, the value of C_{dl} would be taken at the frequency where the phase is close to –90°, but a comparison of the experimental data with the simple lumped circuit model in Fig. 2 shows the experimental phase deviating from the approach to -90°. The deviation from -90° makes it difficult to pick the best frequency for determining the value of C_{dl}. In fact C_{dl} appears to be somewhat frequency dependent; some reasons for this effect appear in the discussion below. As expected, C_{dl} also increases with increasing temperature, due to the greatly increased conductivity of the film and changing microstructure near the crystal melting temperature.

More drastic changes in C_{dl} are observed in response to high concentrations of particular analytes. Fig. 10 shows the impedance spectra, taken at 22°C, for a PEO_7 film for a wide range of relative humidity. At high relative humidity the value of C_{dl} increases, as shown by the decreasing impedance and theta value approaching -90° in the low frequency regime. . Note the problem that can occur when choosing a measurement frequency for this class of sensor. In the data of Fig. 10, is clear that a sampling frequency appropriate to sample the value of R_{ionic} for dry N_2 would be completely inappropriate for measurement of R_{ionic} at a relative humidity of 90%. For example, a sampling frequency of 100 Hz would sample the flat region of the dry N_2 curve but would be dominated by the sloped portion of the curve resulting from the double layer capacitance at a humidity of 90%. Conversely, if the sampling frequency were set to optimum for 90% humidity (200 kHz), the response of dry N_2 would be hidden by the effect of the parasitic capacitance.

Fig. 11 shows impedance spectrum for a dry PEO 7:1 film and two analytes with concentrations selected to give a very similar ionic conductivity, for direct comparison with the double layer region of the spectra. The range of measurement in these impedance spectra was also extended to very low frequencies (10^{-4} Hz) to aid in the comparison. The structure in the impedance spectra in the low frequency region led us to explore the possibility that the C_{dl} could be used to identify particular analytes.

Discussion

Mechanism of Ionic Conductivity

Mechanisms concerning ionic conductivity in PEO have been under intense discussion for over 20 years.[2] It has proved to be much more complicated than ions diffusing in a liquid. In PEO at room temperature there may exist as many as three different phases with different amounts of salt dissolved in them: 1) the polymer amorphous phase (the glass transition temperature, T_g, for this phase is about 200 K); 2) the polymer crystalline phase (melts at about 330 K) and 3) an ion pair crystal complex with PEO (melts at about 400K). Many experiments in the literature show that the measured bulk conductivity occurs mostly in the polymer amorphous phase. In the amorphous phase, above T_g, the ionic conductivity is found to be strongly thermally activated[2], but usually curved when plotted in the typical Arrhenius fashion, as our data in Fig. 6 for the amorphous film. This behavior is often modeled by the so-called VTF equation [2] , which has the form:

$$\ln(\sigma) = A\exp(-E_a/(T-T_0)), \text{ with } A = \sigma_0/T^{1/2} \qquad [2]$$

where E_a is the apparent activation energy and T_0 is a critical temperature, usually associated with the T_g. The equation gives a very steep dependence with temperature as T approaches T_0, and at higher temperatures, the dependence follows a more Arrhenius-like behavior, with an activation energy equal to E_a. Absorbed analytes can affect the conductivity in two ways in this mechanism, by lowering the value of T_0, E_a, or both. Lowering T_0 has the effect of plasticizing the polymer, making the chain segments more flexible. This can also be seen to lower the viscosity of the medium, which affects ion mobility in regular liquids. Ions can also move in solid media by hopping over an energy barrier. The analyte could be lowering that barrier by dielectric screening, for example.

Because of the complex phase behavior of PEO, the analyte could also be increasing the fraction of the amorphous phase, or even increasing the number of mobile ions by affecting the ion pairing. A number of publications[2,9-11] describe the increase in the bulk ionic conductivity by the addition of plasticizers (usually non-volatile compounds), but no model is presented which would allow the calculation of the sensitivity of the conductivity to concentration of analyte. Such a calculation would require a model of the role of chemical structure of the analyte in lowering the glass transition temperature of the polymer, or the other mechanisms, in addition to the solubility of the analyte in the polymer at different pressures and temperatures. The VTF model is probably a good approximation for the temperature dependence of the conductivity in the amorphous film in Fig. 6, but the very steep dependence of the conductivity of the same film with a high crystallite volume fraction must be due to other mechanisms. The effect can not just be the reduced volume fraction of the amorphous phase, because then the temperature dependence would look just like the amorphous film curve, translated down in conductivity by a constant factor, of about 300. There would then be a huge increase in conductivity at the melting point of the crystalline regions. It appears that the fraction of amorphous phase is increasing more gradually from 300 to 340 K; this concept is confirmed by NMR measurements that distinguish protons in the crystalline phase from the amorphous.[2,12] Comparing the several order of magnitude increase in dry conductivity over the small 300 to 340 K temperature range with the order of magnitude increase in conductivity at 300K for low concentrations of some analytes (Fig. 3) points to a percolation mechanism dominating the conductivity in this region.[13] In this model the conductivity in the "flat" frequency range in Fig. 2 is being dominated by high resistance regions in the sample, for example a narrow neck or channel of amorphous polymer between two or more crystallites. These regions are sometimes referred to "tortuous paths".[2,7] Mathematical models of percolation[13] show that small changes in volume fraction of the conducting phase can lead to large changes in conductivity if the system is close to the percolation limit, that is, close to closing down all conduction paths across the whole film, electrode to electrode.

Ionic Conductivity and Analyte Solubility Parameter

In a previous publication[6] we discussed the role of the solubility parameters of various analytes in predicting the response of chemiresistor sensors based on a wide variety of polymer hosts. Figs. 3 and 5 show the relative response of PEO based sensors to a wide variety of analytes with different solubility parameters. The value of the solubility parameter gives a qualitative measure of the absorbed mass of analyte molecule into the polymer as a function of the partial pressure of the analyte[6,14]. In general, an analyte whose solubility parameter is close to the polymer solubility parameter will give a bigger signal (larger change in film resistance) than one where the solubility parameters differ greatly. The PEO ion conductors respond to polar analytes like methanol, ethanol and water in much the same manner as the polar polymer chemiresistors like polyvinylalcohol (PVA).[6] They also show very little response to non-polar analytes like isooctane. However, there are certain molecules, such as DIMP and DMMP that show extraordinarily large responses in the crystalline PEO ion conductors. In Fig. 5 it can be seen that carbon composite chemiresistors made from PEG do not have the extra large relative response to DIMP and DMMP that the ion-conducting counterpart has. We believe that these differences come from the different mechanisms for detecting the presence of the absorbed analyte molecules. For carbon composite chemiresistors, the swelling of the polymer gives the increased resistance[6], while the ion conductors are responding to more subtle effects of the analyte molecule than just swelling, including melting of crystalline regions of the polymer and the effect on polymer chain segmental motions. Unfortunately, the modeling[2] of the behavior of these "plasticizer" molecules has not proceeded to the point of predicting the effect of different molecular structures (like DIMP vs. methanol) on the detailed ion motion leading to conductivity changes. This model is further supported by the results in Fig. 12, where the observed responses at 21°C from the *amorphous* film to the same concentration of six of the common analytes are more than 10 times smaller (comparing fractional changes in conductivity) than from the *crystalline* films . In other words, if there are no crystals to melt, the analyte is only affecting the other parameters, such as the T_g , viscosity and ion pair association, by swelling the film.

Crystalline and Amorphous Phases of PEO and the Temperature Dependence of Conductivity

Most of the data shown in this paper are for films with an easily observed crystalline phase at ambient temperature. Spherulites can be seen with a polarizing microscope. The mixed crystal and amorphous phases are the most common form of films of this material. However it is possible to form a completely amorphous film by heating past the melting temperature of the polymer/salt complex, about 140°C. When cooled back down to ambient temperatures, the recrystallization time is unpredictable. We were able to measure the response of one sensor that stayed amorphous for more than eight weeks, while others have reported recrystallization to occur after only a few days.[2,15] We were also able to cycle between 21°C and 70°C (the melting point of pure PEO crystals) without causing recrystallization. The increase in ionic conductivity for the amorphous sample vs. its crystalline form is very large, roughly a factor of 300 at 21°C. Fig. 1 of Ref. 2 shows this hysteresis effect as reported by another author[15]. Fig. 12 shows the response to solvents like on the amorphous sensor. The fractional change in resistance was much smaller for all the solvent vapors (by a factor of 60, for example, for 10% relative humidity) compared to the responses shown in Fig. 3. The signal to noise was quite good, but the small baseline drift combined with the small signal showed us that the only advantage to having an all-amorphous-phase sensor was the lower base resistance (about 10 kohms at 10 kHz); this would make inexpensive read-out electronics somewhat simpler.

The fact that the fractional change in resistance for the same analyte concentration is much smaller than in the mixed crystalline/amorphous phase tells us that the sensing mechanism is not just controlled by the volume of the amorphous material in a particular sensor. In that case, the fractional signal change would stay the same, identical to making the sensing film thinner. The very large responses shown in Fig. 3 further support the proposed mechanism where the analyte molecules cause some melting, or dissolution of the crystalline phase, particularly in the highly resistive "necks" of amorphous polymer between crystals. In this way the addition of, for example, 10% relative humidity, in Fig. 3a mimics an increase in temperature of about 10 degrees in Fig. 6.

Speed of Response

The data in Fig. 3 gives the speed of response for pulses of a number of analytes at three different temperatures. For example, the 90% of full signal level for H_2O at 21°C is 40 seconds, which reduces to 30 seconds at 39°C. The desorption is almost as fast in most cases, with the exception of a "tail" for large signals like DIMP at 21°C. These fast responses are typical for vapor diffusing into thin polymer films (around 0.5 microns in this case). The actual sensor response time may be somewhat faster than what is shown here, because of the time the whole vapor flow system takes to deliver the correct concentration of the analyte to the sensor. This delay can include adsorption of analyte molecules on tubing walls. Many measurements of diffusion rates in thin polymer films are given in a book on acoustic wave devices.[14] It is perhaps surprising that the responses of the PEO crystalline polymers are as fast as we observe; it is thought that the diffusion constants are much smaller in the crystalline phase of a polymer.

The Double Layer Region of the Impedance Spectrum

The simplest model of the electrical double layer was worked out almost 90 years ago and is described in textbooks.[16] The application was an attempt to understand aqueous electrolytes with various ions, concentrations, electrode materials and potentials, etc. In spite of the success of the early models in describing the gross aspects of the double layer capacitance, like its magnitude, in many cases prominent details of the spectra (as function of electrode potential) go unexplained. In our case with gold electrodes and a $LiClO_4$ electrolyte it is expected that the interface is "perfectly polarizable". That is, no electrochemical charge transfer takes place between the electrode and the electrolyte. Examples of redox reactions using solid polymer electrolytes are given in several references, where redox species are purposely introduced and the currents due to charge transfer are measured.[17] In our case, the very large impedance values shown in Fig. 2 at low frequencies are indicative of double layers of ions formed on "blocking" or "polarizable" electrodes. This kind of capacitance is not due to a thin layer of dielectric material where charges (ions or electrons) reside only on the surfaces of the dielectric and no charges move inside the dielectric; that is the simplest kind of parallel plate capacitor. With ions that can move, as shown by the ionic conductivity part of the impedance spectrum, a more complicated kind of capacitance occurs where there is a thermally mediated balance between the spatial distribution of concentrations of the mobile ions (both positively and negatively charged species). A voltage drop is caused by the charge separation (differences in concentration of ions with charges of opposite sign) near the electrode. In especially clean electrode/electrolyte systems[16], the predictions of the simple double layer model concerning the absolute magnitude of the capacitance, the steep voltage dependence of that capacitance, and the dependence on ion concentration are confirmed. However, many complications usually cause substantial deviations from those predictions as is well documented over the many years of study of this phenomenon. For solid polymer electrolytes there have been few studies of the double layer capacitance.[18,19] In a carefully executed experiment, Bruce and his colleagues measured the double layer capacitance from a cross-linked PEO to a movable liquid mercury electrode. They were able to introduce a Li reference electrode so they could measure and control the potential on the mercury during the capacitance measurement, including frequency dependence. The magnitude of the capacitance, about 10 microfarads/cm^2, agrees in general with our measurements, however we were not able to measure and control our electrode potentials. We do not apply a DC bias during our measurements, so both sets of gold electrode fingers are at the same resting potential; this means we do not have an absolute measure of that potential. In any case the careful measurements in Ref. 18 do not show the expected potential or ionic concentration dependencies, and speculation about mechanisms causing these deviations are given.

Our first goal in examining the double layer part of the impedance spectrum was to determine if the magnitude or frequency dependence was influenced by the type of analyte molecule. A sufficiently distinctive fingerprint could allow us to identify an analyte and determine its concentration with a single sensor. We reasoned that since the measured double layer impedance spectrum reflects the structure of the mobile ions and the polymer very near the electrode, there could be a signature dependence [19] on the analyte molecules that would be independent of the analyte concentration, which as shown above, often has a very strong affect on the ionic conductivity. Ideally, following the lumped circuit in Fig. 2, each analyte would have a different C_2 value, which would be independent of the ionic conductivity, represented by R_{ionic}. Unfortunately, the double layer region of the impedance spectrum is more complicated than can be represented by a single C_2 value. The spectrum shown in Fig. 11 gave us some hope that picking the correct frequencies to measure impedance would allow us to distinguish water from DIMP. However, the spectra in Figures 9 and 10 show that the C_2 value does depend on concentration, particularly at high concentrations. After examing a large number of double layer impedances for various analytes at various concentrations, we can not find a sufficiently useful correlation between the double layer capacitance (at any frequency) and any of the analytes to use for identification.

Conclusions

In summary, polymeric ionic conductors are excellent candidates for low power, small size chemiresistors to be used for detecting volatile organic compounds, including water. They have particular patterns of response to different analytes, which compliment chemiresistors fabricated from other polymers and using different analyte detection mechanisms. Arrays of such chemiresistors can be used to identify various VOC's and to identify complex vapor mixtures when used in electronic noses with pattern recognition algorithms.

In the case of PEO we have identified a new chemical detection mechanism in mixed crystalline/amorphous phase films: the absorbed analyte molecules can reversibly melt or dissolve some of the crystal phase at the edges, increasing the volume for ion conductivity through narrow channels between the large spherulitic crystals. This mechanism produces very large fractional changes in conductivity, by increasing the size and number of the percolation channels for ion conduction, when most of the film volume is occupied by the (non-conducting) crystalline phases. The measured double layer capacitance values at low frequencies show unusual dependencies on the analytes and their concentrations, but have not provided sufficient correlation to use as means of identifying analytes.

Acknowledgements

Sandia is a multiprogram laboratory operated by Sandia Corporation, a Lockheed Martin Company, for the United States Department of Energy under Contract DE-AC04-94AL85000. We would like to thank Mark Jenkins of Sandia for excellent technical assistance.

References

1. E. Quartarone, P. Mustarelli, and A. Magistris, *Solid State Ionics*, **110**, 1 (1998).
2. M. Ratner, in *Polymer Electrolyte Reviews*, vol. 1, J. R. MacCallum and C. Vincent, eds., p. 173, Elsevier, London (1987).
3. S. L. Garverick and S. D. Senturia, *IEEE Trans. Electron Devs.*, **29**, 90 (1982).
4. R. C. Hughes, M. P. Eastman, W. G. Yelton, A. J. Ricco, S. V. Patel, and M. W. Jenkins, *Digest of the State Sensor and Actuator Workshop*, Hilton Head, SC, June 1998,pp. 379-382, Transducers Research Foundation, Cleveland (1998).
5. P. V. Gerwen, W. Laureys, G. Huyberechts, M. Beeck, K. Baert, J. Suls, A. Varlan, W. Sandsen, L. Hermans, and R. Mertens, *Transducers '97 Digest of the 1997 International Conference on Solid State Sensors and Actuators*, Transducers '97, pp. 907-910, Chicago, Ill., June 16-19,1997, (1997).
6. M. P. Eastman, R. C. Hughes, W. G. Yelton, A. J. Ricco, S. V. Patel, and M. W. Jenkins, *J. Electochem. Soc.*, **146**, 3907 (1999).
7. P. Bruce, in *Polymer Electrolyte Reviews*, vol. 1, J. R. MacCallum and C. Vincent, eds., p. 237, Elsevier, London (1987).
8. R. P. Janek, W. R. Fawcett, and A. Ulam, *J. Phys. Chem. B*, **101**, 8550 (1997).
9. A. M. Sukeshini, A. R. Kulkarni, and A Sharma, *Solid State Ionics*, **115**, 179 (1998).
10. R. Frech and S Chintapalli, *Solid State Ionics*, **85**, 61 (1996).
11. N. Binesh and S. V. Bhat, *Solid State Ionics*, **122**, 291 (1999).
12. C. Berthier, W. Gorecki, M. Minier, M. B. Armand, J. M. Chabagno, and P. Rigaud, *Solid State Ionics*, **11**, 91 (1983).

13. B. Lundberg and B. Sundqvist, *J. Appl. Phys.*, **60**, 1074 (1986).

14. D. S. Ballantine, R. M. White, S. J. Martin, A. J. Ricco, E. T. Zellers, G. C. Frye, H. Wohltjen, *Acoustic Wave Sensors: Theory, Design and Physico-Chemical Applications,* Chapters 4 and 5, Academic Press, Inc., San Diego, CA (1997).

15. S. M. Ansari, M. Brodwin, M. Stainer, S. D. Druger, M. A. Ratner, and D. F. Shriver, *Solid State Ionics*, **17**, 101 (1985).

16. A. W. Adamson, *Physical Chemistry of Surfaces*, 3rd ed., chap. IV, John Wiley & Sons, New York (1976).

17. L. Geng, M. L. Longmire, R. A. Reed, J. F. Parcher, C. J. Barbour, and R. W. Murray, *Chem. Mater.,* **1**, 58 (1989).

18. P. G. Bruce, E. S. McGregor, and C. A. Vincent, *Electrochim. Acta*, **37**, 1525 (1992).

19. K. B. Pfeifer, R. C. Hughes, M. W. Jenkins, and T. W. Schneider, *J. Electrochem. Soc.*, **146**, 794 (1999).

Figure Captions

Figure 1. PEO film on interdigitated electrodes showing crystallites. Polarizing filters were used to emphasize the appearance of the crystallites.

Figure 2. Comparison of PEO impedance data with lumped circuit model

Figure 3. Responses to P/P_{sat} = 10% of 11 different solvents at a) 21°C, b) 39°C, and c) 59°C. The impedance was measured at 100 Hz with a 0.5 V AC oscillation potential and no DC bias. The phase shifts were also measured during the exposures but are not shown. Analysis of the frequency spectra using the lumped circuit model is required to obtain an accurate value of R_{ionic} in the presence of the solvents giving large signals. However, in this case we wish to show the temporal response characteristics of the sensor using a simple read-out circuit.

Figure 4. Transient and steady state responses of $PEO_{15}(LiClO_4)$ to various concentrations of DIMP. Two different sensor temperature were used, but the DIMP bubbler was kept at 21°C. The profile of the DIMP concentrations (1 ppm $\approx$1% P/P_{sat})from the flow controllers is shown by the dashed lines and the right hand scale.

Figure 5 Relative responses to P/P_{sat} = 10% of 12 solvents in order of increasing solubility parameter form left to right. Responses for the $PEG68_{10}(LiClO_4)$ device are presented as $\log(G/G_0)$, and for the PEG68-30-C device as $\Delta R/R_0$.

Figure 6. Thermal characteristics of the ionic impedance of a semi-crystalline and amorphous phase $PEO_{15}(LiClO_4)$ device. The thermal profile was first measured on the semi-crystalline film, then the device was heated to 140°C and quenched to room temperature to create the fully amorphous phase.

Figure 7. Four-Terminal dc resistance measurements during heating to 91°C and then cooling of a PEG68-30-C sensor in N_2. The hysteresis is indicative of super-cooling of the amorphous form before crystallites reformed.

Figure 8. AC impedance measurements at 100 Hz in N_2 during heating to 91°C and then cooling to 20°C. The semi-crystalline form of PEG68 shows large impedance shifts with relatively small temperature changes, however, once in the amorphous form, at high temperatures, the change in impedance is much smaller.

Figure 9. Impedance spectra of $PEO_{10}(LiClO_4)$ at 21°C in N_2 and in various acetonitrile concentrations. The ionic impedance is a strong function of analyte concentration.

Figure 10. Impedance spectra at 22°C for $PEO_7(LiClO_4)$ in N_2 and in various percentages of relative humidity.

Figure 11. Impedance spectra for $PEO_7(LiClO_4)$ at 22°C. Even for analyte exposures where the ionic impedance is identical the double layer capacitance varies at lower frequencies. This suggests a method for chemical identification. Note that for the two analytes, the value of the

phase angle is different at 10^5 Hz even though the ionic impedance is nearly identical. Both theta and |Z| spectra have features that may aid in distinguishing the analytes.

Figure 12. Amorphous phase $PEO_{15}(LiClO_4)$ responses to 6 solvents (P/P_{sat} = 10% for each solvent) are significantly smaller than the same solvent exposures on a semi-crystalline device. The solvents and sensor were at 21°C, and the sensor was measured at 1000 Hz.

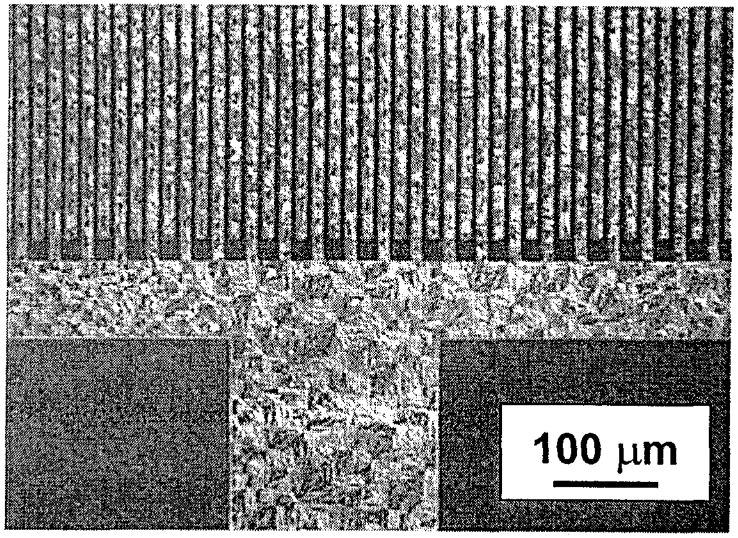

Figure 1

Figure 2

Measured and Simulated Frequency Spectra

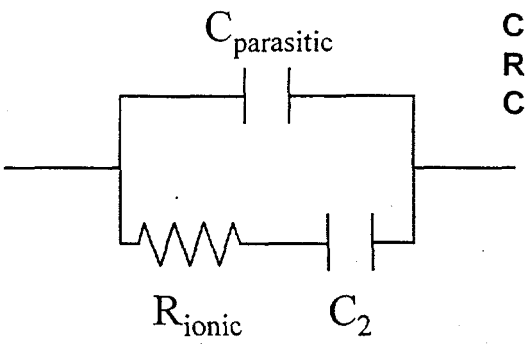

Fit Parameters	N_2 simulated	20% RH simulated
$C_{parasitic}$	8.7×10^{-11} F	8.7×10^{-11} F
R_{ionic}	$2.0 \times 10^{7}\ \Omega$	$4.8 \times 10^{5}\ \Omega$
C_2	1.0×10^{-8} F	2.9×10^{-8} F

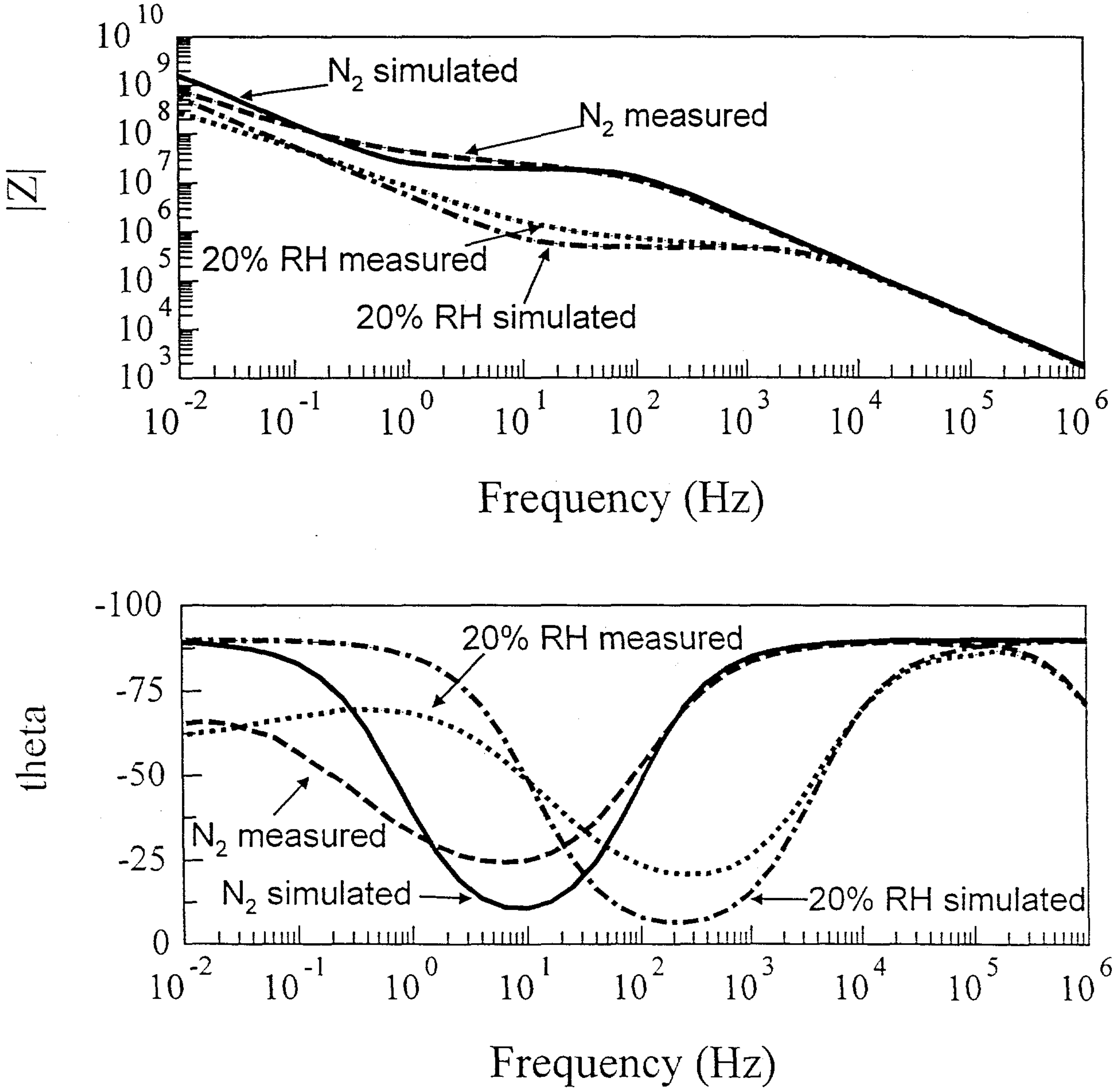

Figure 3

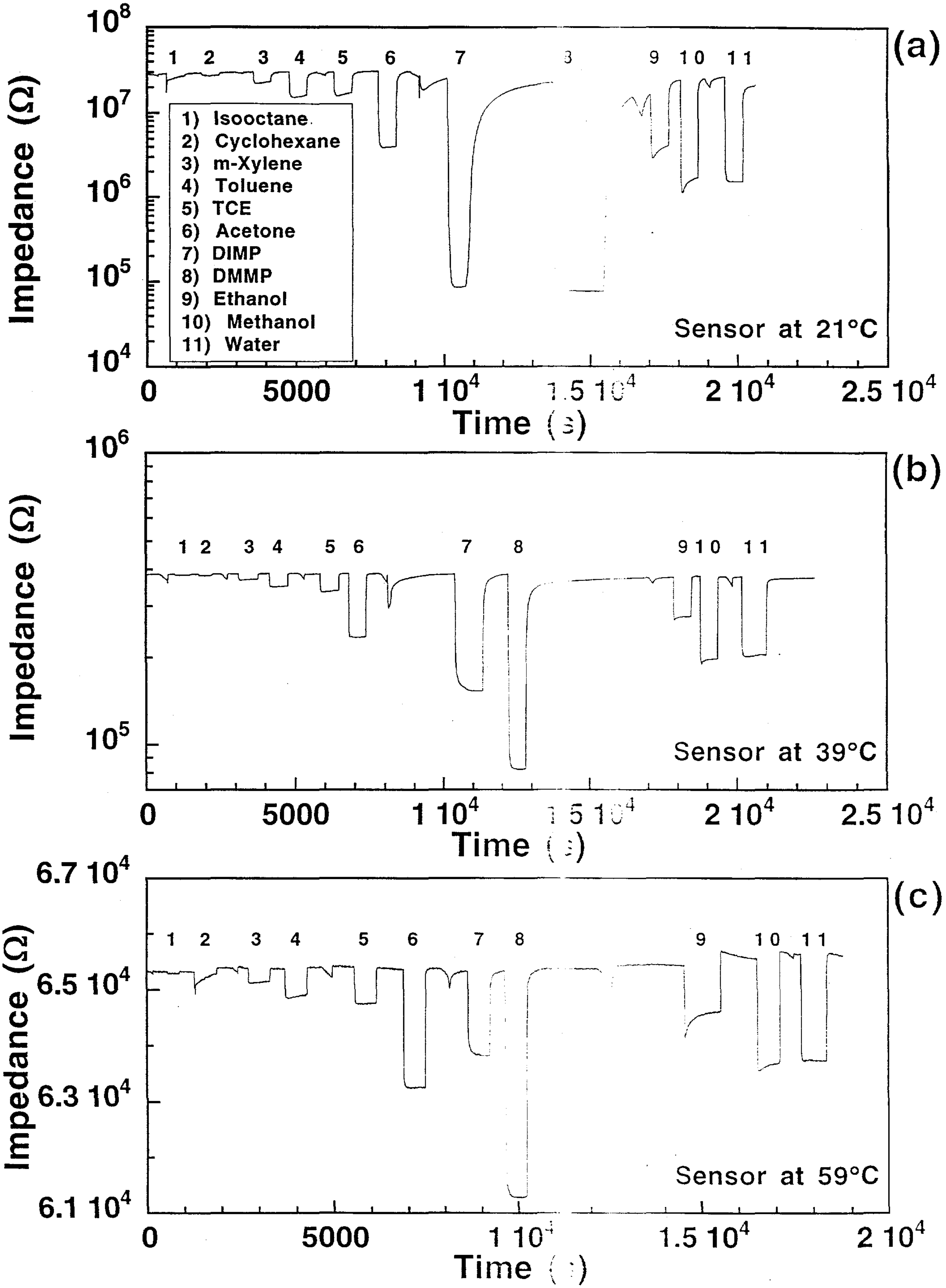

(a)
Impedance (Ω)
10^8
10^7
10^6
10^5
10^4
1 2 3 4 5 6 7 8 9 10 11
1) Isooctane
2) Cyclohexane
3) m-Xylene
4) Toluene
5) TCE
6) Acetone
7) DIMP
8) DMMP
9) Ethanol
10) Methanol
11) Water
Sensor at 21°C
0
5000
1 10^4
1.5 10^4
2 10^4
2.5 10^4
Time (s)
(b)
Impedance (Ω)
10^6
10^5
1 2 3 4 5 6 7 8 9 10 11
Sensor at 39°C
0
5000
1 10^4
1.5 10^4
2 10^4
2.5 10^4
Time (s)
(c)
Impedance (Ω)
6.7 10^4
6.5 10^4
6.3 10^4
6.1 10^4
1 2 3 4 5 6 7 8 9 10 11
Sensor at 59°C
0
5000
1 10^4
1.5 10^4
2 10^4
Time (s)

Figure 4

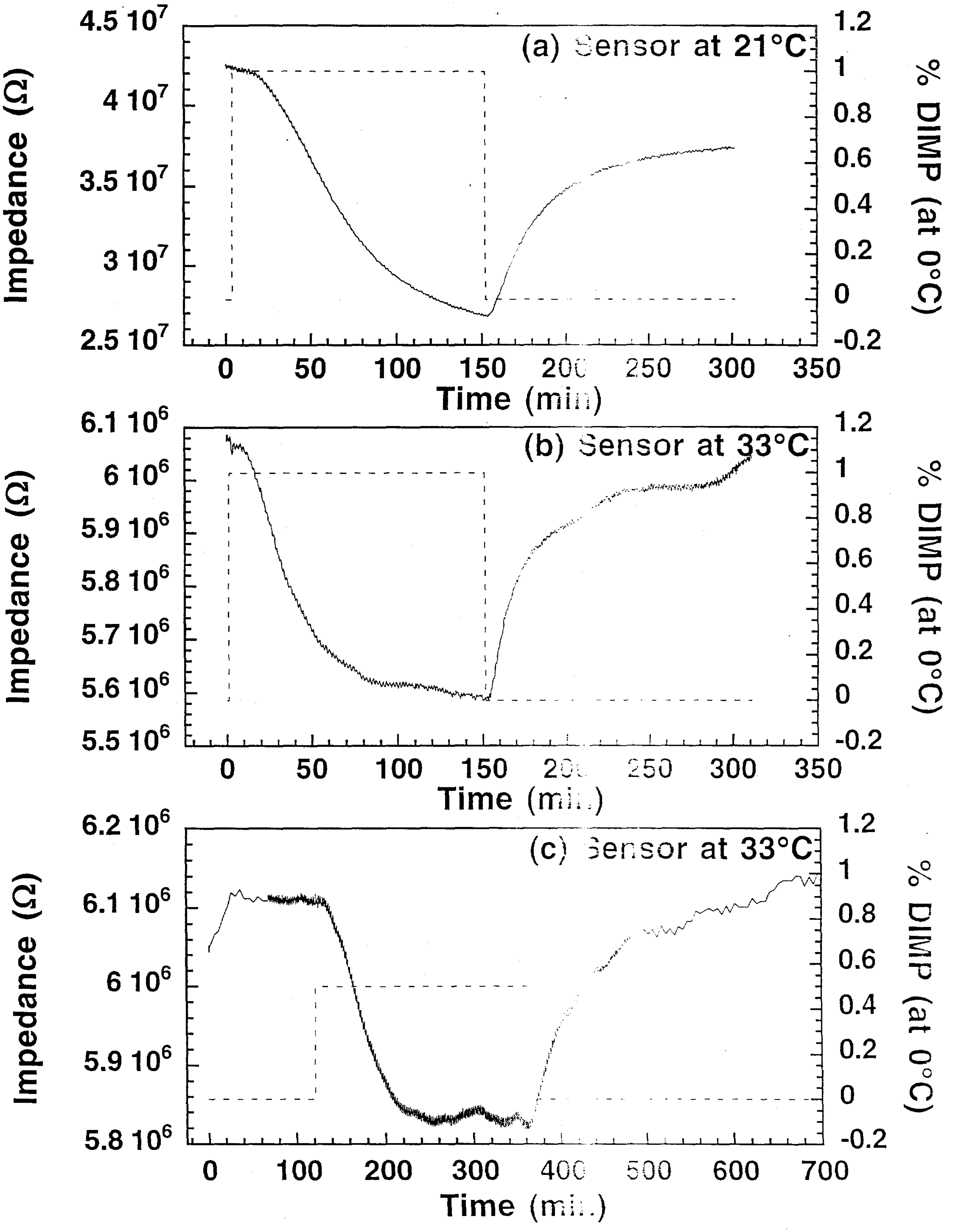
(a) Sensor at 21°C
Impedance (Ω)
4.5 10^7
4 10^7
3.5 10^7
3 10^7
2.5 10^7
% DIMP (at 0°C)
1.2
1
0.8
0.6
0.4
0.2
0
-0.2
0
50
100
150
200
250
300
350
Time (min)
(b) Sensor at 33°C
Impedance (Ω)
6.1 10^6
6 10^6
5.9 10^6
5.8 10^6
5.7 10^6
5.6 10^6
5.5 10^6
% DIMP (at 0°C)
1.2
1
0.8
0.6
0.4
0.2
0
-0.2
0
50
100
150
200
250
300
350
Time (min)
(c) Sensor at 33°C
Impedance (Ω)
6.2 10^6
6.1 10^6
6 10^6
5.9 10^6
5.8 10^6
% DIMP (at 0°C)
1.2
1
0.8
0.6
0.4
0.2
0
-0.2
0
100
200
300
400
500
600
700
Time (min)

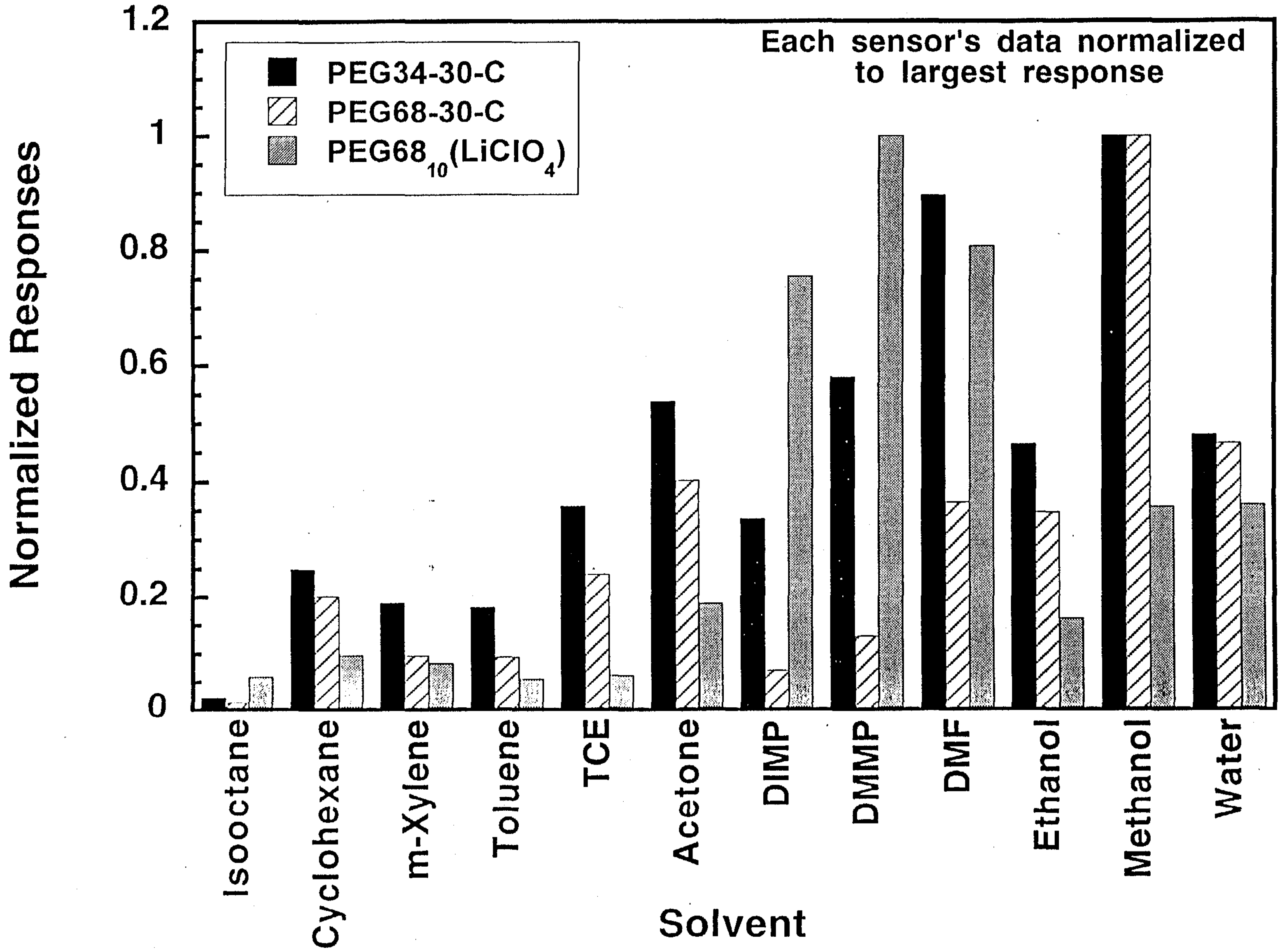

Each sensor's data normalized to largest response
PEG34-30-C
PEG68-30-C
PEG68$_{10}$(LiClO$_4$)
Normalized Responses
1.2
1
0.8
0.6
0.4
0.2
0
Isooctane
Cyclohexane
m-Xylene
Toluene
TCE
Acetone
DIMP
DMMP
DMF
Ethanol
Methanol
Water
Solvent

Figure 5

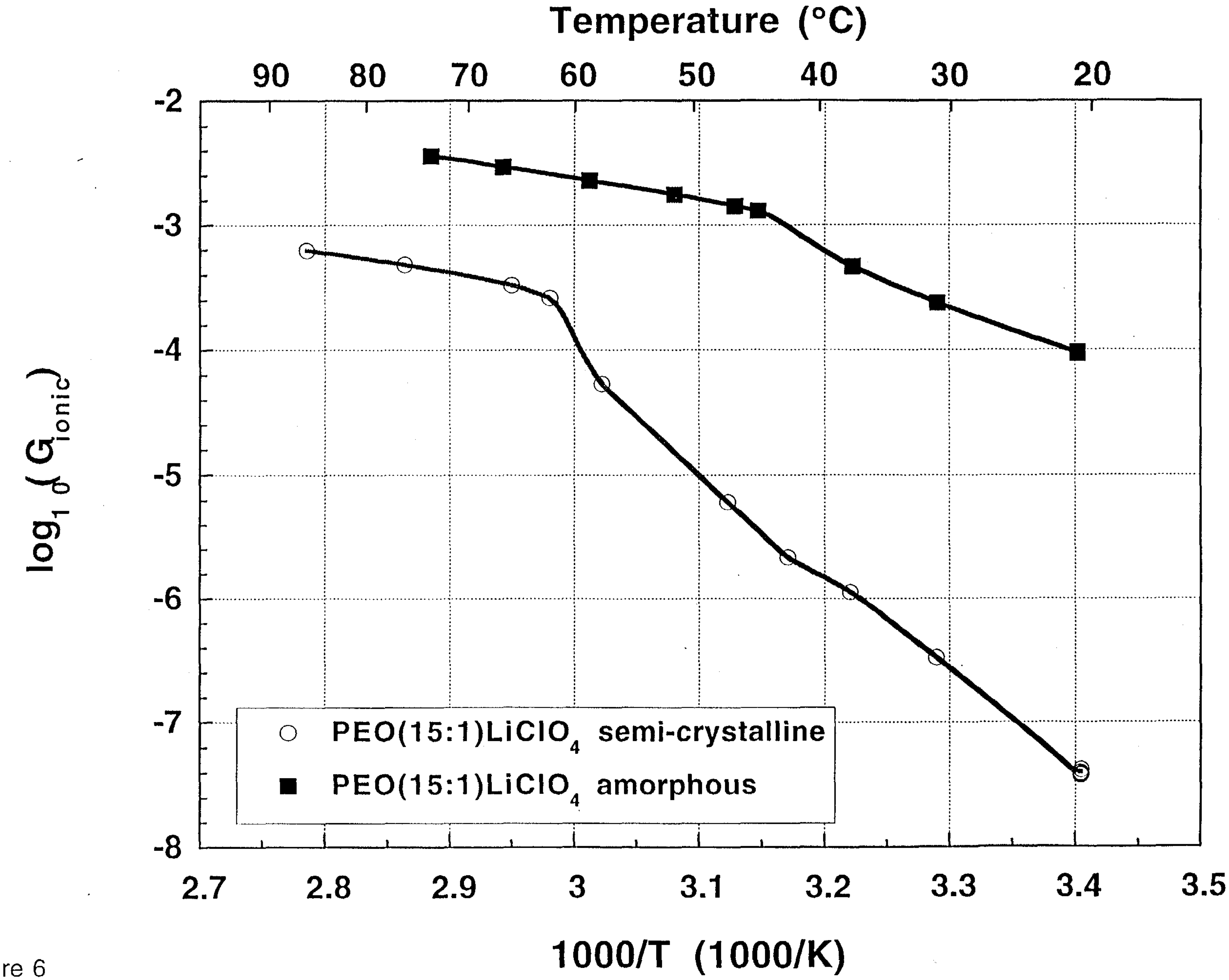
Temperature (°C)
90
80
70
60
50
40
30
20
-2
-3
-4
-5
-6
-7
-8
$\log_{10}(G_{ionic})$
2.7
2.8
2.9
3
3.1
3.2
3.3
3.4
3.5
1000/T (1000/K)
○ PEO(15:1)$LiClO_4$ semi-crystalline
■ PEO(15:1)$LiClO_4$ amorphous

Figure 6

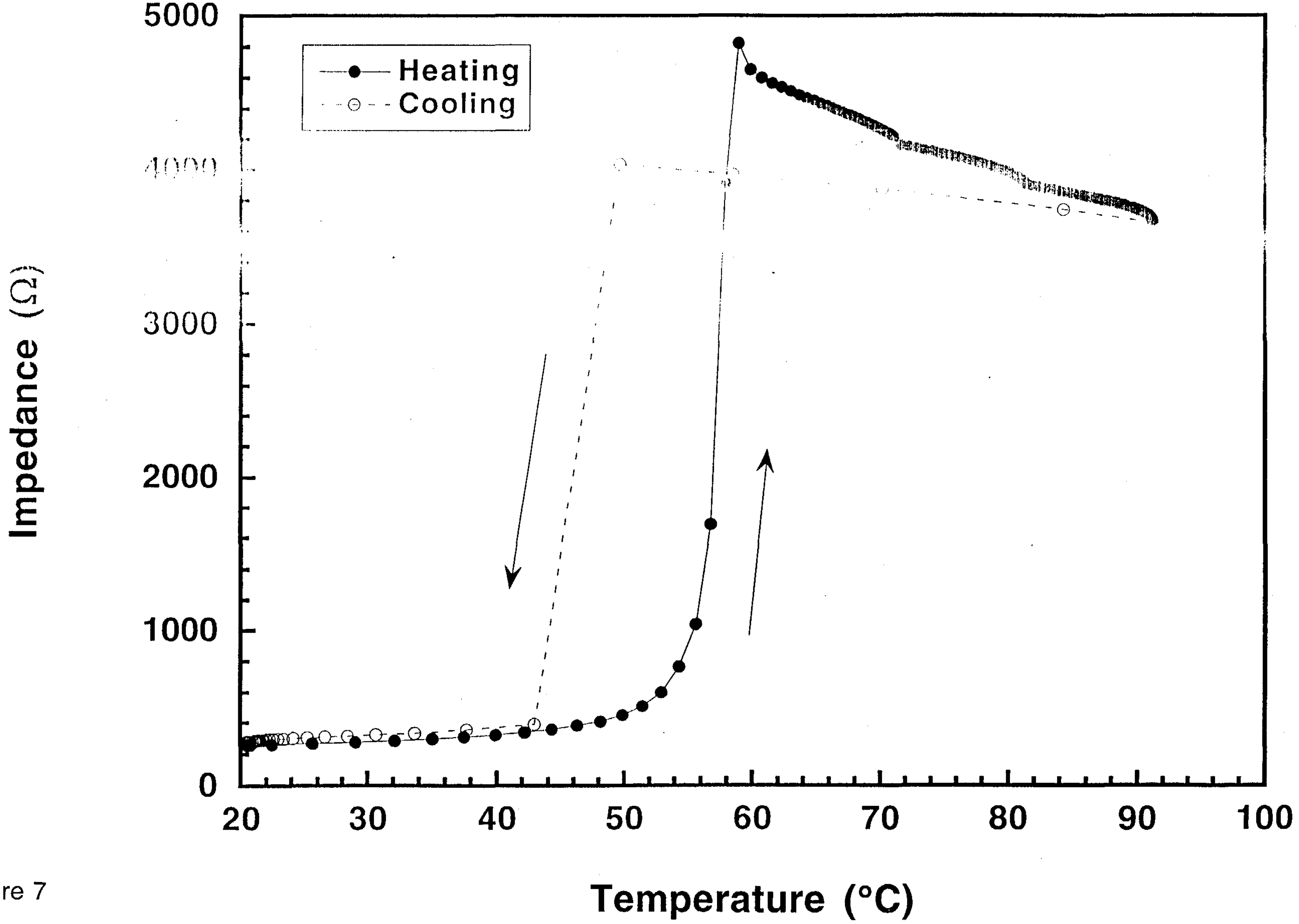
Heating
Cooling
5000
4000
3000
2000
1000
0
20
30
40
50
60
70
80
90
100
Impedance (Ω)
Temperature (°C)

Figure 7

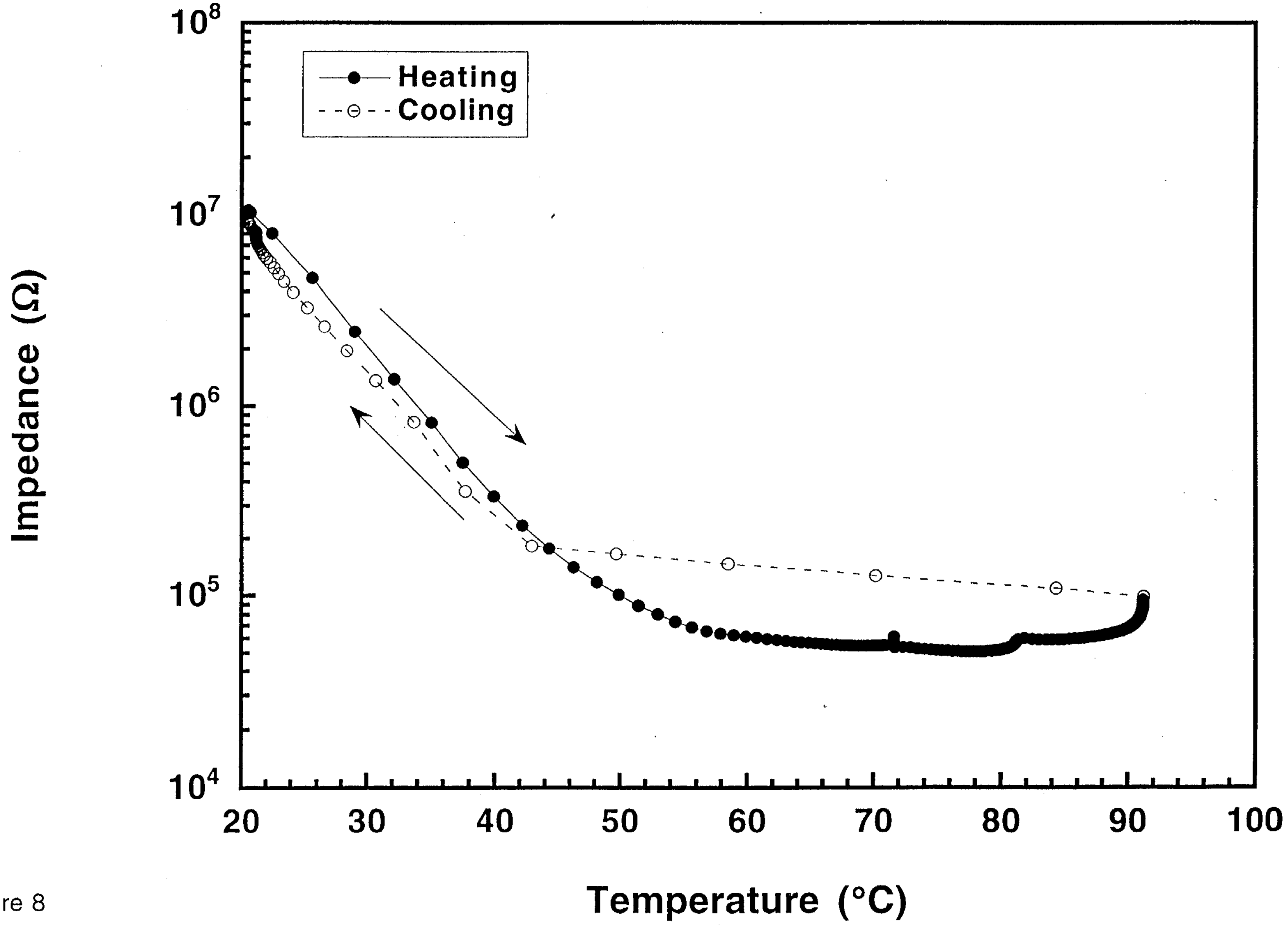
Heating
Cooling
Impedance (Ω)
10^8
10^7
10^6
10^5
10^4
20
30
40
50
60
70
80
90
100
Temperature (°C)

Figure 8

Figure 9

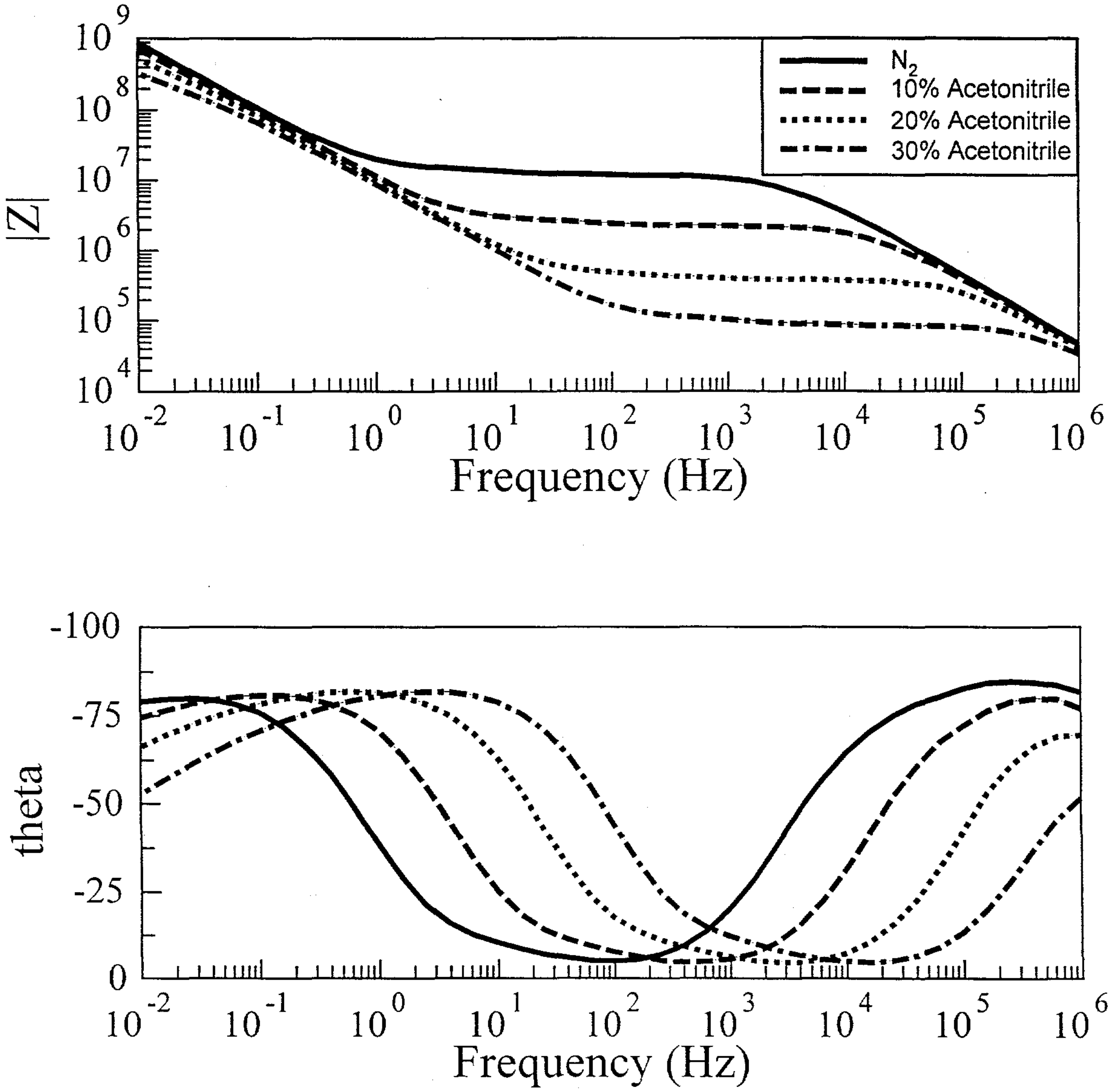

10^9
10^8
10^7
10^6
10^5
10^4
|Z|
N_2
10% Acetonitrile
20% Acetonitrile
30% Acetonitrile
10^{-2}
10^{-1}
10^0
10^1
10^2
10^3
10^4
10^5
10^6
Frequency (Hz)
-100
-75
-50
-25
0
theta
10^{-2}
10^{-1}
10^0
10^1
10^2
10^3
10^4
10^5
10^6
Frequency (Hz)

Figure 10

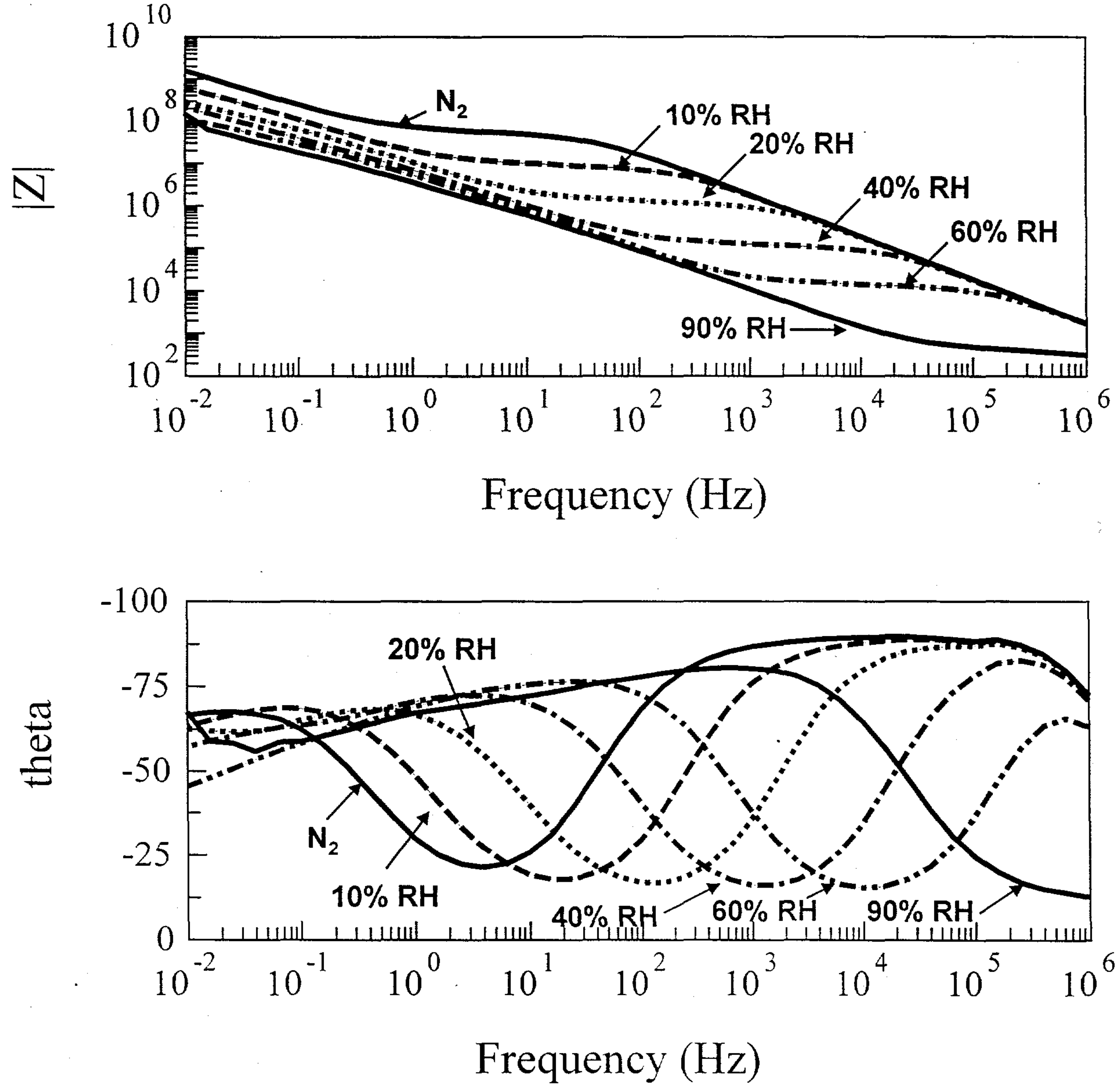

|Z|
10^10
10^8
10^6
10^4
10^2
N2
10% RH
20% RH
40% RH
60% RH
90% RH
10^-2
10^-1
10^0
10^1
10^2
10^3
10^4
10^5
10^6
Frequency (Hz)
theta
-100
-75
-50
-25
0
20% RH
N2
10% RH
40% RH
60% RH
90% RH
10^-2
10^-1
10^0
10^1
10^2
10^3
10^4
10^5
10^6
Frequency (Hz)

Figure 11

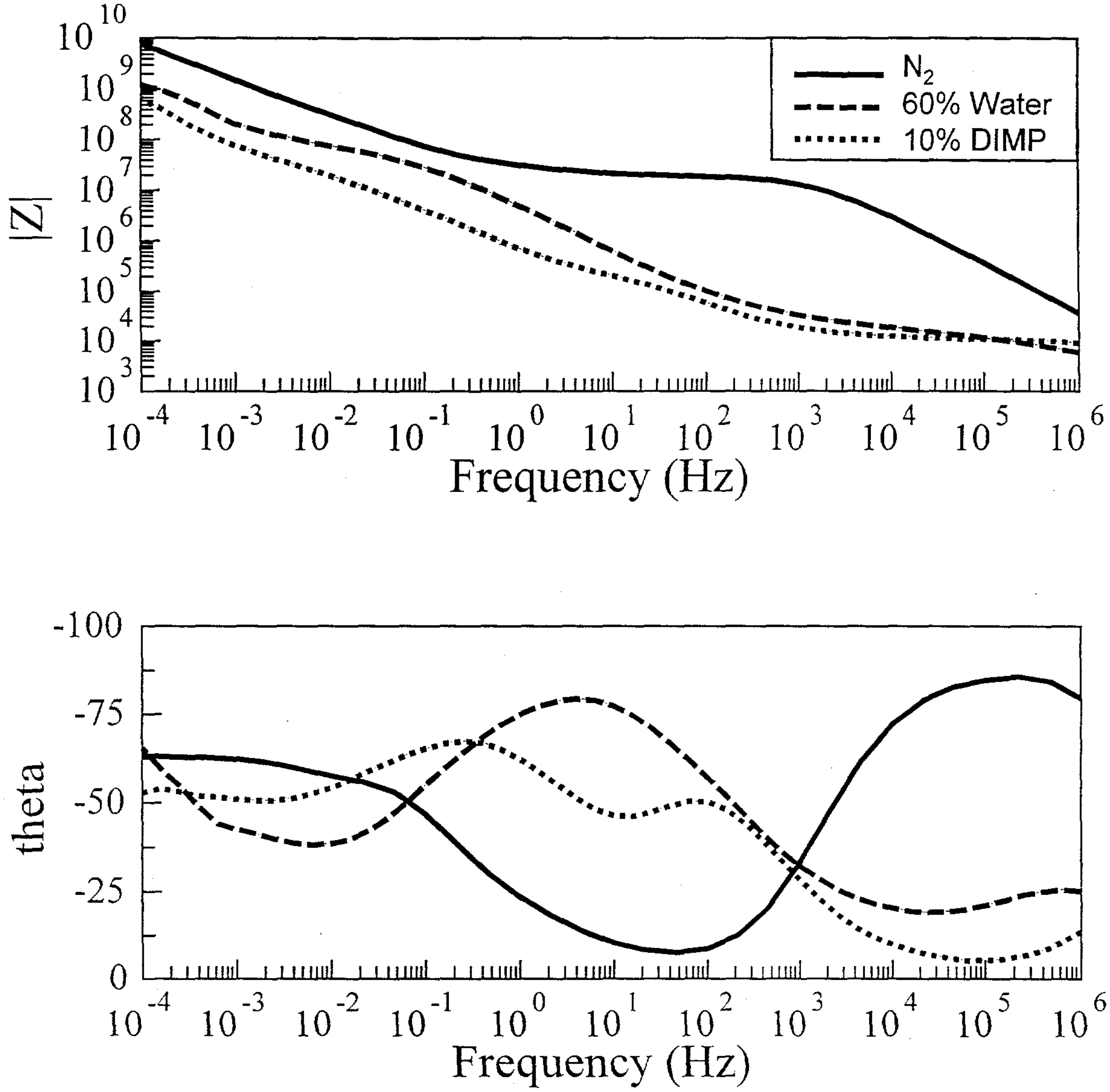
N_2
60% Water
10% DIMP
|Z|
10^{3}
10^{4}
10^{5}
10^{6}
10^{7}
10^{8}
10^{9}
10^{10}
theta
0
-25
-50
-75
-100
10^{-4}
10^{-3}
10^{-2}
10^{-1}
10^{0}
10^{1}
10^{2}
10^{3}
10^{4}
10^{5}
10^{6}
Frequency (Hz)

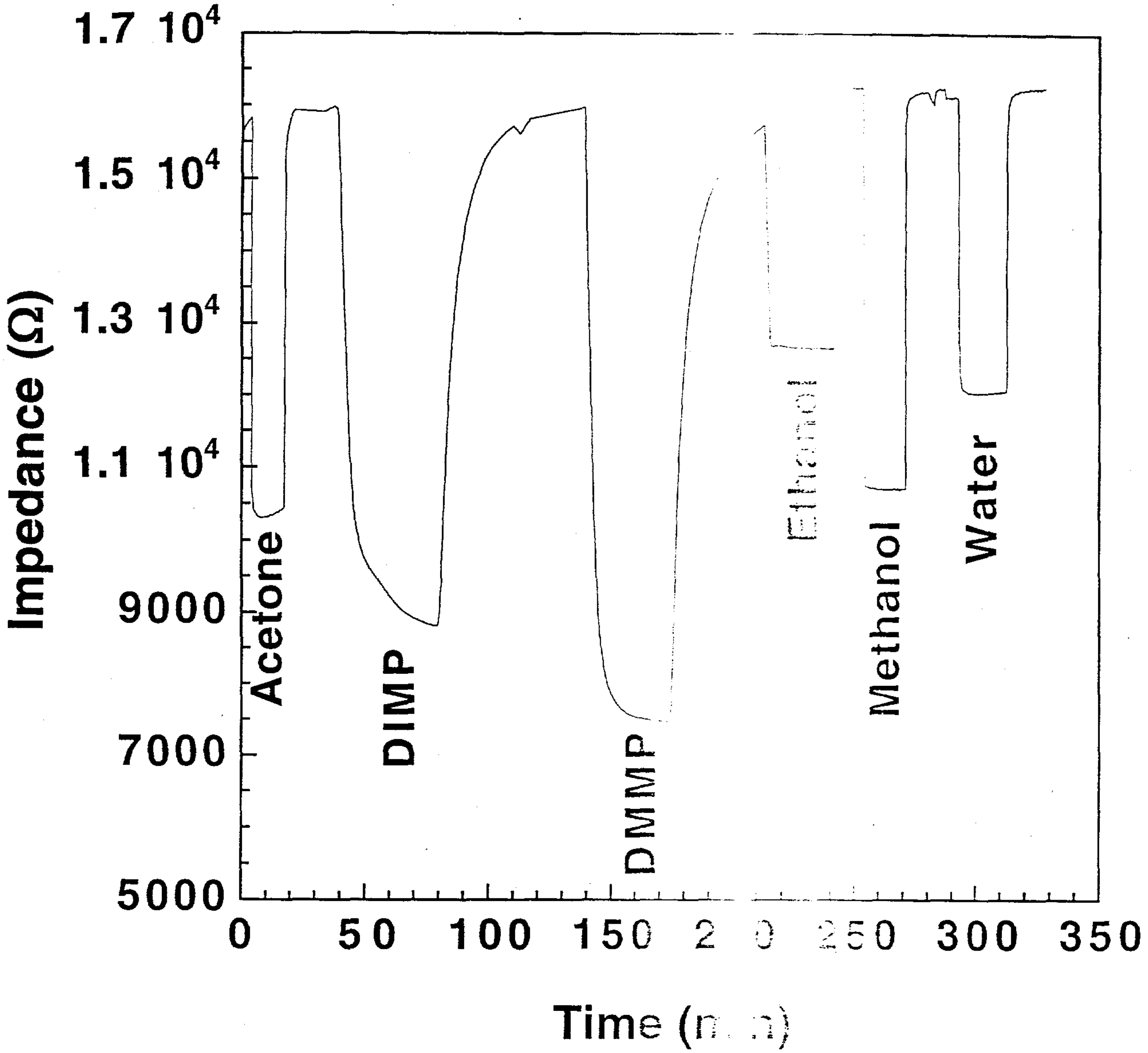
Impedance (Ω)
1.7 10^4
1.5 10^4
1.3 10^4
1.1 10^4
9000
7000
5000
Acetone
DIMP
DMMP
Ethanol
Methanol
Water
0
50
100
150
200
250
300
350
Time (min)

Figure 12

MANUSCRIPT CHECKLIST

Report/Manuscript SAND-

Author/Org: R. C. Hughes, et al

Title: "Characteristics and Mechanisms in Ion-Conducting ....."

Journal/ Meeting: J. Electrochem. Soc

* * * * * * * * * * * * * * * *

		Org.	Initial	Date
Reviewer:		[illegible]	R.J.	5/31/2000
Reviewer:				

Comments:

① Experimental section might require a more detailed description of methods

1. Concentrations of PEO in AN used to coat electrodes
2. Exact method of coating electrodes and geometry of device
3. How was thickness of polymer measured?
4. Was there a difference between spin or drop coated

② Please include comments/data regarding error and standard deviation in the numerical values presented in this paper.